Statistics of a confined, randomly accelerated particle with inelastic boundary collisions

Theodore W. Burkhardt, Jerrold Franklin, and Richard R. Gawronski
Department of Physics, Temple University, Philadelphia, Pennsylvania 19122

(Received 30 September 1999; revised manuscript received 30 November 1999)

We consider the one-dimensional motion of a particle randomly accelerated by Gaussian white noise on the line segment $0<x<1$. The reflections of the particle from the boundaries at $x=0,1$ are inelastic. The velocities just before and after reflection are related by $v_f=-rv_i$, where r is the coefficient of restitution. Cornell, Swift, and Bray [Phys. Rev. Lett. **81**, 1142 (1998)] have argued that there is an inelastic collapse transition in this system. For $r>r_c=e^{-\pi/\sqrt{3}}$ the particle moves throughout the interval $0<x<1$, while for $r<r_c$ the particle is localized at $x=0$ or $x=1$. In this paper the equilibrium distribution function $P(x,v)$ is analyzed for $r>r_c$ by solving the steady-state Fokker-Planck equation, and the results are compared with numerical simulations.

PACS number(s): 05.10.Gg, 02.50.Ey, 05.40.−a

I. INTRODUCTION

Consider a particle moving in one dimension on the semi-infinite line $x>0$ according to the Langevin equation

$$\frac{d^2x}{dt^2}=\eta(t). \tag{1}$$

The acceleration $\eta(t)$ has the form of Gaussian white noise, with mean $\langle\eta(t)\rangle=0$ and correlation function $\langle\eta(t_1)\eta(t_2)\rangle=2\delta(t_1-t_2)$. The collisions of the particle with the boundary at $x=0$ are inelastic. The velocities v_i and v_f just before and after the collision are related by $v_f=-rv_i$, where r is the coefficient of restitution.

This model, which may be relevant to clustering in driven granular matter and the Brownian motion of colloids, has recently been studied by Cornell, Swift, and Bray [1,2]. Their most striking conclusion is that the system exhibits ''inelastic collapse.'' For r less than a critical value

$$r_c=e^{-\pi/\sqrt{3}}=0.1630\ldots \tag{2}$$

the inelastic particle in the half space $x>0$ makes infinitely many boundary collisions in a finite time and becomes localized at $x=0$. Cornell *et al.* argue that a particle confined to the finite interval $0<x<1$ undergoes a similar transition. It moves throughout the interval for $r>r_c$ and is localized at $x=0$ or 1 for $r<r_c$, with the same value r_c as for the half space.

In this paper we consider the equilibrium statistical properties of the randomly accelerated inelastic particle on the interval $0<x<1$. The equilibrium distribution function $P(x,v)$ for the position and velocity of the particle satisfies the steady-state Fokker-Planck equation [1]

$$\left(v\frac{\partial}{\partial x}-\frac{\partial^2}{\partial v^2}\right)P(x,v)=0 \tag{3}$$

corresponding to Eq. (1) with the boundary conditions

$$P(x,v)=P(1-x,-v), \tag{4}$$

$$P(0,-v)=r^2P(0,rv),\quad v>0, \tag{5}$$

implied by reflection symmetry and conservation of probability [3], respectively. In Sec. II we show how to solve Eqs. (3)–(5) for $r>r_c$ with a Green's function appoach. Both analytical and numerical results for $P(x,v)$ are presented. Some of these results are compared with simulations in Sec. III. Section IV contains concluding remarks.

II. SOLUTION OF THE FOKKER-PLANCK EQUATION

Our analytical approach to calculating $P(x,v)$ was inspired by Masoliver and Porrà [4], who solved a related Fokker-Planck equation in deriving the mean escape time of a randomly accelerated particle from the interval $0<x<1$. The central ingredient in our work is a Green's function solution of Eq. (3),

$$P(x,v)=\frac{v^{1/2}}{3x}\int_0^\infty du\,u^{3/2}e^{-(v^3+u^3)/9x}I_{-1/3}\left(\frac{2v^{3/2}u^{3/2}}{9x}\right)P(0,u)$$
$$-\frac{1}{3^{1/3}\Gamma(\frac{2}{3})}\int_0^x dy\,\frac{e^{-v^3/9(x-y)}}{(x-y)^{2/3}}\,\frac{\partial P(y,0)}{\partial v} \tag{6}$$

that determines $P(x,v)$ for all $x>0$, $v>0$ from the boundary values $P(0,v)$ and $\partial P(x,0)/\partial v$. The quantity $I_\nu(z)$ in Eq. (6) is the usual modified Bessel function [5,6]. We emphasize that Eq. (6) only holds for positive v. $P(x,v)$ for negative v can be obtained from Eq. (6) using reflection symmetry (4).

A detailed derivation of Eq. (6) is given in Appendix A. By substituting Eq. (6) into Eq. (3), it is simple to check that the differential equation is indeed satisfied. Equation (6) is also consistent on the lines $x=0$ and $v=0$. In the limit $x\to 0$ both the right-hand and left-hand sides approach $P(0,v)$, as follows from the asymptotic form $I_\nu(z)\approx(2\pi z)^{-1}e^z$ for large z. On differentiating Eq. (6) with respect to v and then taking the limit $v\to 0$, both the right and left sides approach $\partial P(x,0)/\partial v$.

There are two unknown functions $P(0,v)$ and $\partial P(x,0)/\partial v$ on the right-hand side of Eq. (6). Imposing the requirement (4) of reflection symmetry on the solution (6), we show in Appendix B that the the second unknown function is related to the first by

$$\frac{\partial P(x,0)}{\partial v}=\int_0^\infty du\, u[R(x,u)-R(1-x,u)]P(0,u), \quad (7)$$

where

$$R(x,u)=\frac{1}{3^{5/6}\Gamma(\frac{1}{3})\Gamma(\frac{5}{6})}\frac{u^{1/2}e^{-u^3/9x}}{x^{7/6}(1-x)^{1/6}} \times {}_1F_1\left(-\frac{1}{6},\frac{5}{6},\frac{u^3(1-x)}{9x}\right), \quad (8)$$

and ${}_1F_1(a,b,z)$ is the confluent hypergeometric function [5–7]. Equations (6)–(8), which still involve one unknown function $P(0,v)$, formally solve the Fokker-Planck equation for any boundary condition (see, for example, Ref. [8]) at $x=0,1$ consistent with the reflection symmetry (4).

Imposing the inelastic boundary condition (5) on the solution (6) yields an integral equation that determines $P(0,v)$ for the randomly accelerated inelastic particle. From Eqs. (4) and (5), $r^2P(0,rv)=P(1,v)$ for $v>0$. Rewriting the right-hand side of this relation using Eq. (6), we obtain

$$r^2P(0,rv)=\frac{v^{1/2}}{3}\int_0^\infty du\, u^{3/2}e^{-(v^3+u^3)/9} \times I_{-1/3}(\tfrac{2}{9}v^{3/2}u^{3/2})P(0,u) + \frac{1}{3^{1/3}\Gamma(\frac{2}{3})}\int_0^1 dy\, y^{-2/3}e^{-v^3/9y}\frac{\partial P(y,0)}{\partial v}. \quad (9)$$

Here the integration variable in the second integral has been changed from y to $1-y$, using

$$\frac{\partial P(y,0)}{\partial v}=-\frac{\partial P(1-y,0)}{\partial v}, \quad (10)$$

which follows from Eq. (4).

Next we eliminate $\partial P(y,0)/\partial v$ from Eq. (9) using Eqs. (7),(8) and integrate over y with the help of [6]. This yields an integral equation for the function

$$g(z)=v^{-1/2}P(0,v), \quad z=v^3/9 \quad (11)$$

given by

$$g(r^3z)=\frac{1}{2\pi r^{5/2}}\int_0^\infty dz'\, e^{-(z+z')} \times\left[\frac{1}{z+z'}+6\,{}_1F_2(1;\tfrac{5}{6},\tfrac{7}{6};zz')\right]g(z'), \quad (12)$$

where ${}_1F_2(a;b,c;z)$ is a generalized hypergeometric function [6,7]. The key step in calculating $P(x,v)$ is solving integral equation (12) for $g(z)$. Once $g(z)$ has been determined, $P(0,v)$ follows from Eq. (11) and $P(x,v)$ from the integrals in Eqs. (6)–(8).

In the case $r=1$ of elastic boundary collisions, Eq. (12) has the solution $g(z)=\text{const}\times z^{-1/6}$, implying $P(0,v)=\text{const}$ and, from Eqs. (6)–(8), $P(x,v)=\text{const}$. This $P(x,v)$ clearly satisfies the Fokker-Planck equation (3) with boundary conditions (4) and (5). Since $P(x,v)$ is independent of v, the equilibrium average of the kinetic energy is infinite. According to the Langevin equation (1), the mean kinetic energy at time t is given, for $r=1$, by

$$\tfrac{1}{2}\langle v(t)^2\rangle=\tfrac{1}{2}v(0)^2+t, \quad r=1, \quad (13)$$

which also diverges in the limit $t\to\infty$.

The asymptotic behavior of $P(0,v)$ for small and large v is determined by the first and second terms, respectively, of the kernel in integral equation (12). For small v the first term is dominant, and we find

$$P(0,v)\sim v^{-\beta(r)}, \quad 0<v\ll 1, \quad (14)$$

where the exponent $\beta(r)$ depends on r according to

$$r=\left\{2\sin\left[(2\beta+1)\frac{\pi}{6}\right]\right\}^{1/(\beta-2)}. \quad (15)$$

For large v the second term of the kernel is dominant. Making use of ${}_1F_2(1;\frac{5}{6},\frac{7}{6};z)\approx\frac{1}{6}\pi^{1/2}z^{-1/4}\exp(2z^{1/2})$ for large positive z, we find

$$P(0,v)\sim\exp[-v^3/v_{\rm ch}(r)^3], \quad v\gg 1, \quad (16)$$

where the characteristic velocity $v_{\rm ch}(r)$ is given by

$$v_{\rm ch}(r)^3=\frac{9r^3}{1-r^3}. \quad (17)$$

As r decreases, the boundary collisions become more inelastic. The probability of finding the particle near the boundary with a small velocity increases. This is reflected in the monotonic increase of $\beta(r)$ with decreasing r and the monotonic decrease of $v_{\rm ch}(r)$, apparent from Eqs. (15),(17). As r decreases from 1 to 0, $\beta(r)$ increases from 0 to $\frac{5}{2}$. The integral equation (12) for $P(0,v)$ has a well defined solution for $0\leqslant\beta<\frac{5}{2}$. However, for β greater than the critical value $\beta_c=2$, the two integrals in Eq. (6) diverge. Thus our solution to the Fokker-Planck equation breaks down for $\beta>\beta_c$ or $r<r_c$. From Eq. (15) one sees that $\beta_c=2$ corresponds to the critical value $r_c=e^{-\pi/\sqrt{3}}$. This is the same as the critical value (2) for the inelastic collapse transition found by Cornell, Swift, and Bray [1]

To solve integral equation (12) for $g(z)$, we remove the leading singularity at $z=0$ by introducing the function

$$f(z)=z^\alpha e^z g(r^3z), \quad \alpha=\frac{1}{6}(2\beta+1). \quad (18)$$

The corresponding integral equation for $f(z)$ can then be written as

$$f(z)=1+\frac{r^{1/2}}{2\pi}\int_0^\infty dz'\, z'^{-\alpha}e^{-(1+r^3)z'} \times[K(z,z')-K(1,z')]f(z'), \quad (19)$$

with the kernel

$$K(z,z')=z^\alpha\left[\frac{1}{z+r^3z'}+6\,{}_1F_2(1;\tfrac{5}{6},\tfrac{7}{6};r^3zz')\right]. \quad (20)$$

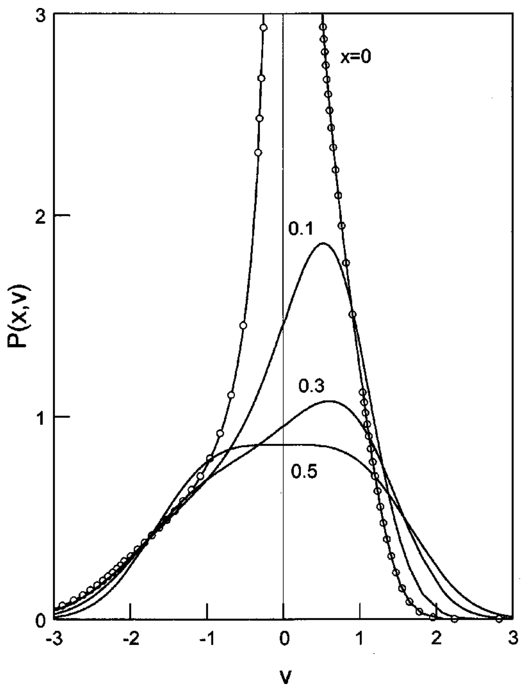

FIG. 1. The function $P(x,v)$ (solid lines) for $r=\frac{1}{2}$ obtained by solving the integral equation (12) for $P(0,v)$, $v>0$ and integrating Eqs. (6)–(8) numerically, making use of reflection symmetry (4). As discussed in the text, the points shown by empty circles confirm that the numerical results for $P(x,v)$ do indeed satisfy the inelastic boundary condition (5).

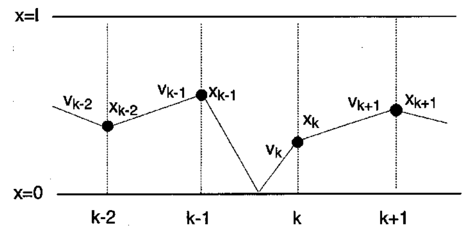

FIG. 2. Schematic trajectory of the simulated particle. The particle travels with constant velocity between kicks, except when it strikes the boundary and is reflected inelastically. Our simulations were performed with gentle kicks to approximate the continuous dynamics, and the corresponding trajectories are much smoother than shown.

Here $f(z)$ has been normalized so that $f(1)=1$ by introducing a subtracted kernel. This permits solution by iteration, which would not work for the original homogeneous integral equation. The boundary velocity distribution $P(0,v)$, obtained from the numerical solution of integral equation (19) and Eqs. (11) and (18), is compared with results from simulations in the next section.

Once $P(0,v)$ is known, $P(x,v)$ follows, for positive v, from integration according to Eqs. (6)–(8) and, for negative v, from reflection symmetry (4). For $r_c<r<1$, $P(x,v)$ is a nonsingular function of (x,v) except at the two boundary points (0,0) and (1,0). On approaching these points at constant $x=0$ or 1, $P(x,v)$ diverges as $A|v|^{-\beta(r)}$, as in Eqs. (14),(15), with different amplitudes A for positive and negative v, consistent with the inelastic boundary condition (5). On approaching the singular points at constant $v=0$, $P(x,v)$ diverges as $x^{-\beta(r)/3}$ for $x\to 0$ and as $(1-x)^{-\beta(r)/3}$ for $x\to 1$, as follows from Eqs. (6)–(8).

Carrying out the integrals in Eqs. (6)–(8) numerically for $r=\frac{1}{2}$, we obtain the function $P(x,v)$ shown in Fig. 1. The divergence at $v=0$ and the asymmetry between v and $-v$, due to the asymmetric inelastic boundary condition (5), are apparent on the curve for $x=0$ in Fig. 1. On the curves for $x=0.1$, 0.3, and 0.5 the divergence is replaced by a rounded peak. The peak becomes broader and more symmetric as x increases. The asymmetry disappears at $x=0.5$, as required by reflection symmetry (4).

The solid curve for $P(0,v)$, $v<0$ in Fig. 1 was obtained from our numerical solution of the integral equation (12) for $P(0,v)$, $v>0$ by integrating Eqs. (6)–(8) numerically to obtain $P(1,v)$, $v>0$ and then using reflection symmetry (4). The functions $P(0,v)$ for $v<0$ and $v>0$ are also directly related by the inelastic boundary condition (5). The points for $P(0,v)$, $v<0$ denoted by empty circles in Fig. 1 were obtained by substituting the points for $P(0,v)$, $v>0$ shown in the figure into Eq. (5). That the points for $P(0,v)$, $v<0$ obtained this way lie right on the corresponding solid curve, as they should, serves as an important check of our numerical work.

As r decreases, $P(x,v)$ becomes more strongly peaked around the most probable values $(x,v)=(0,0),(1,0)$, where $P(x,v)$ diverges. According to our numerical results for $P(x,v)$, the probability of finding the particle at a distance less than 0.1 from the boundary, independent of its velocity, increases from about 32% for $r=0.8$ to 84% for $r=0.2$.

III. COMPUTER SIMULATIONS

We have also carried out computer simulations of a randomly accelerated particle making inelastic boundary collisions. The particle moves on the line $0<x<1$ and receives random kicks at times $t=0,\tau,2\tau,3\tau,\ldots$, resulting in discontinuous velocity changes. Between two consecutive kicks the particle moves with constant velocity except when it strikes the boundary. In this case it is reflected, with its velocity multiplied by $-r$. A sample trajectory is shown in Fig. 2. Denoting the position of the particle as the kth kick is applied by x_k and the velocity *just before* the kth kick by v_k, we write the corresponding equation of motion as

$$v_k=v_{k-1}+\xi_{k-1}, \tag{21}$$

$$x_k=x_{k-1}+v_k\tau, \tag{22}$$

if the particle does not strike the boundary between kicks $k-1$ and k, i.e., if $0<x_{k-1}+v_k\tau<1$. Otherwise these equations are replaced by

$$v_k=-r(v_{k-1}+\xi_{k-1}), \tag{23}$$

$$x_k=\begin{cases}-rx_{k-1}+v_k\tau, & x_{k-1}+v_k\tau<0,\\ (1+r)-rx_{k-1}+v_k\tau, & x_{k-1}+v_k\tau>1.\end{cases} \tag{24}$$

The velocity change ξ_k is selected randomly from a Gaussian distribution, with $\langle\xi_k\xi_{k'}\rangle=2\tau\delta_{k,k'}$. For this distribution

$\frac{1}{2}\langle v_k^2\rangle = \frac{1}{2}v_0^2 + k\tau$ for $r=1$, analogous to Eq. (13). Note that the root-mean-square velocity change is given by $\Delta v_{\rm rms} = \langle \xi_k^2\rangle^{1/2} = (2\tau)^{1/2}$.

The difference equations (21)–(24) provide a good approximation to the differential equation (1) when the relative velocity change per kick is small, i.e., for $\Delta v_{\rm rms} \ll |v|$. The simulations described below were performed with $\Delta v_{\rm rms} = (2\tau)^{1/2} = 0.004$ or $\tau = 8\times 10^{-6}$.

Assuming the equivalence of ensemble averages and long-time averages for a single system, one may estimate $P(x,v)$ and $P(0,v)$ from a single simulation with a large number of steps N using the relations

$$P(x,v) = \frac{1}{N\tau}\int_0^{N\tau} dt\ \delta(x - x(t))\delta(v - v(t)), \qquad (25)$$

$$P(0,v) = \lim_{\Delta\to 0}\frac{1}{\Delta}\int_0^{\Delta} dx\ P(x,v)$$

$$= \lim_{\Delta\to 0}\frac{1}{N\tau\Delta}\int_0^{N\tau} dt\ \theta(\Delta - x(t))\delta(v - v(t)), \quad (26)$$

where θ denotes the standard step function. The distribution function $P(x,v)$ in Eq. (25) is normalized so that

$$\int_0^1 dx \int_{-\infty}^{\infty} dv\ P(x,v) = 1. \qquad (27)$$

Referring to Fig. 2, consider the contribution of the zigzag trajectory from x_{k-2} to x_{k+1} to $P(0,v)$ in Eq. (26). Only the middle interval, which contains a boundary collision, gives a nonvanishing contribution, $(N\tau)^{-1}|v|^{-1}[\delta(v + r^{-1}v_k) + \delta(v - v_k)]$, in the limit $\Delta\to 0$. Note that this contribution explicitly satisfies the inelastic boundary condition (5).

In our simulations $P(0,v)$ was determined by iterating the difference equations $N=10^9$ times and summing the contributions (see the preceding paragraph) of all the boundary collisions. In practice, this involves sorting all the velocities v_k just after boundary collisions in bins $\alpha = 1,2,\ldots$ of width Δv and calculating the number N_α, average $\langle v\rangle_\alpha$, and average inverse $\langle v^{-1}\rangle_\alpha$ of the velocities in bin α. The data points in Fig. 3 show the contributions $P_\alpha, \langle v\rangle_\alpha$ of the various bins, where

$$P_\alpha = \frac{N_\alpha \langle v^{-1}\rangle_\alpha}{N\tau\Delta v}. \qquad (28)$$

Here P_α in Eq. (28) is normalized consistently with $P(x,v)$ in Eq. (27).

The results of our simulations are shown in Fig. 3 for $r=0.2$ (filled circles) and $r=0.8$ (empty circles). The error bars are comparable to the size of the points, except for the highest and lowest velocities, where the error bars are about twice as large. The solid and dashed curves in Fig. 3 show the function $P(0,v)$ for $r=0.2$ and $r=0.8$ obtained by solving integral equation (12) numerically, as discussed following Eq. (20). The normalization of the curves, which is not fixed by the integral equation, has been chosen so that the data points and curves coincide at $\ln(v/v_{\rm ch}) = -1$. The faint straight lines show the power law (14),(15) for small v.

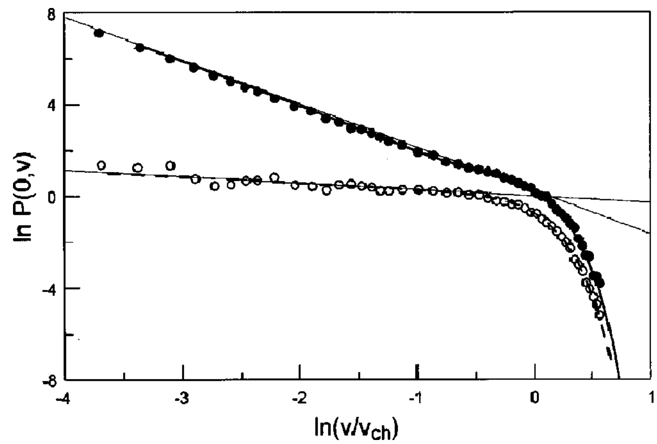

FIG. 3. The boundary probability distribution $P(0,v)$ for $r=0.2$ (solid line) and $r=0.8$ (dashed line) obtained by solving the integral equation (12) numerically. Simulation results for $r=0.2$ (filled circles) and $r=0.8$ (empty circles). The error bars are comparable to the sizes of the circles, except for the highest and lowest velocities, where the error bars are about twice as large. The characteristic velocity $v_{\rm ch}(r)$ is defined in Eq. (17).

The simulation data and the Fokker-Planck results for $P(0,v)$ in Fig. 3 are in excellent agreement. Note that the data extend over nearly six decades in the natural variable v^3 of Eq. (16).

IV. CONCLUDING REMARKS

We have shown how the Fokker-Planck equation for the equilibrium distribution $P(x,v)$ can be solved with a Green's function approach. To obtain $P(x,v)$, we first solve the integral equation (12) for $P(0,v)$ and then substitute the result in Eqs. (6)–(8). A graph of $P(x,v)$ for $r=\frac{1}{2}$, calculated in this way, is shown in Fig. 1.

As discussed following Eq. (17), the Green's function solution exists for $r>r_c$ but not for $r<r_c$, where r_c is the same as the critical value (2) for the inelastic-collapse transition reported by Cornell *et al.* [1,2]. For $r_c<r<1$ the most probable values of (x,v) are (0,0) and (1,0), where $P(x,v)$ is infinite. As r approaches r_c from above, the exponent $\beta(r)$ in the asymptotic form (14),(15) of $P(0,v)$ for small v approaches 2 from below, and the first and second terms on the right-hand side of Eq. (6), which with Eqs. (7),(8) determine $P(x,v)$, diverge positively and negatively, respectively. However, the divergences cancel, and $P(x,v)$ remains normalizable and extended, as opposed to a collapsed delta-function distribution, at $r=r_c$.

Finally we consider the critical behavior of the incident and reflected probability currents

$$I_{\rm inc} = \int_{-\infty}^0 dv\ vP(0,v), \qquad I_{\rm ref} = \int_0^{\infty} dv\ vP(0,v). \qquad (29)$$

Note that these definitions and the inelastic boundary condition (5) imply total current $I_{\rm inc}+I_{\rm ref}=0$, as required for any time-independent distribution. The reflected current is exactly the same as the boundary collision rate. Substituting the small-v behavior (14),(15) of $P(0,v)$ in Eqs. (29) with $\beta(r)\to 2$ as $r\to r_c$ and using the normalizability of $P(x,v)$ at

r_c, we find that the equilibrium boundary collision rate diverges as $(r-r_c)^{-1}$ as r approaches r_c from above. At $r=r_c$ the particle makes an infinite number of collisions with the boundary in a finite time. In their work on inelastic collapse, Cornell *et al.* [1,2] reached a similar conclusion for $r<r_c$.

ACKNOWLEDGMENTS

T.W.B. thanks Gerhard Gompper and co-workers for hospitality at the Institut für Festkörperforschung, Forschungszentrum Jülich and the Alexander von Humboldt Stiftung for financial support.

APPENDIX A: DERIVATION OF EQ. (6)

We begin by extending the finite interval $0<x<1$ to the half line $0<x<\infty$ and introducing the Laplace transform

$$Q(s,v)=\int_0^\infty dx\, e^{-sx}P(x,v), \tag{A1}$$

which according to Eq. (3) satisfies

$$\left(sv-\frac{\partial^2}{\partial v^2}\right)Q(s,v)=vP(0,v). \tag{A2}$$

This differential equation can be solved in terms of standard Airy functions Ai(z),Bi(z), [5], with Wronskian $\mathrm{Ai(z)Bi'(z)-Ai'(z)Bi(z)}=\pi^{-1}$. The solution for positive v that vanishes as $v\to\infty$ is given by

$$\begin{aligned}Q(s,v)=&W(s)\mathrm{Ai}(s^{1/3}v)\\&+\pi s^{-1/3}\left[\mathrm{Bi}(s^{1/3}v)\int_v^\infty du\,\mathrm{Ai}(s^{1/3}u)uP(0,u)\right.\\&\left.+\mathrm{Ai}(s^{1/3}v)\int_0^v du\,\mathrm{Bi}(s^{1/3}u)uP(0,u)\right].\end{aligned} \tag{A3}$$

The quantity $W(s)$ in Eq. (A3) is an arbitrary weight function. It can be expressed in terms of $\partial Q(s,0)/\partial v$ by differentiating Eq. (A3) with respect to v and then setting $v=0$. Substituting the resulting expression for $W(s)$ in Eq. (A3) yields

$$\begin{aligned}Q(s,v)=&s^{-1/3}\frac{\mathrm{Ai}(s^{1/3}v)}{\mathrm{Ai}'(0)}\left[\frac{\partial Q(s,0)}{\partial v}-\pi\mathrm{Bi}'(0)\right.\\&\left.\times\int_0^\infty du\,\mathrm{Ai}(s^{1/3}u)uP(0,u)\right]\\&+\pi s^{-1/3}\left[\mathrm{Bi}(s^{1/3}v)\int_v^\infty du\,\mathrm{Ai}(s^{1/3}u)uP(0,u)\right.\\&\left.+\mathrm{Ai}(s^{1/3}v)\int_0^v du\,\mathrm{Bi}(s^{1/3}u)uP(0,u)\right].\end{aligned} \tag{A4}$$

Next we evaluate the inverse Laplace transform of Eq. (A4), using $\mathcal{L}^{-1}\{Q(s,v)\}=P(x,v)$, the Faltung theorem [9], and the relations

$$\mathrm{Ai}'(0)=-3^{-1/2}\mathrm{Bi}'(0)=-3^{-1/3}\Gamma(\tfrac{1}{3})^{-1},$$

$$\mathcal{L}^{-1}\{s^{-1/3}\mathrm{Ai}(s^{1/3}v)\}=(2\times 3^{1/6}\pi)^{-1}x^{-2/3}e^{-v^3/9x}, \tag{A5}$$

$$\begin{aligned}\mathcal{L}^{-1}&\{s^{-1/3}\mathrm{Ai}(s^{1/3}v)\mathrm{Ai}(s^{1/3}u)\}\\&=(2\times 3^{3/2}\pi)^{-1}x^{-1}(vu)^{1/2}e^{-(v^3+u^3)/9x}\\&\times\left[I_{-1/3}\left(\frac{2(vu)^{3/2}}{9x}\right)-I_{1/3}\left(\frac{2(vu)^{3/2}}{9x}\right)\right],\end{aligned} \tag{A6}$$

$$\begin{aligned}\mathcal{L}^{-1}&\{s^{-1/3}\mathrm{Ai}(s^{1/3}v)\mathrm{Bi}(s^{1/3}u)\}\\&=(6\pi)^{-1}x^{-1}(vu)^{1/2}e^{-(v^3+u^3)/9x}\\&\times\left[I_{-1/3}\left(\frac{2(vu)^{3/2}}{9x}\right)+I_{1/3}\left(\frac{2(vu)^{3/2}}{9x}\right)\right].\end{aligned} \tag{A7}$$

Equations (A5)–(A7) follow from the substitutions [5]

$$\mathrm{Ai}(z)=\frac{z^{1/2}}{3}\left[I_{-1/3}\left(\frac{2}{3}z^{3/2}\right)-I_{1/3}\left(\frac{2}{3}z^{3/2}\right)\right], \tag{A8}$$

$$\mathrm{Bi}(z)=\left(\frac{z}{3}\right)^{1/2}\left[I_{-1/3}\left(\frac{2}{3}z^{3/2}\right)+I_{1/3}\left(\frac{2}{3}z^{3/2}\right)\right], \tag{A9}$$

on the left-hand sides of Eqs. (A5)–(A7) and Ref. [10]. The inverse Laplace transform of Eq. (A4) is the Green's function solution (6) that we set out to prove.

APPENDIX B: DERIVATION OF EQS. (7) AND (8)

In the limit $v\to 0$ Eq. (6) reduces to

$$\begin{aligned}P(x,0)=&\frac{1}{3^{1/3}\Gamma(\frac{2}{3})}\left[x^{-2/3}\int_0^\infty du\,ue^{-u^3/9x}\,P(0,u)\right.\\&\left.-\int_0^x\frac{dy}{(x-y)^{2/3}}\frac{\partial P(y,0)}{\partial v}\right],\end{aligned} \tag{B1}$$

where the form $I_\nu(x)\approx\Gamma(\nu+1)^{-1}(z/2)^\nu$ for small z has been used. From reflection symmetry (4), $P(x,0)-P(1-x,0)=0$. Substituting Eq. (B1) in this relation and using Eq. (10), we obtain

$$\begin{aligned}\int_0^1&\frac{dy}{|x-y|^{2/3}}\frac{\partial P(y,0)}{\partial v}\\&=\int_0^\infty du\,u\left[\frac{e^{-u^3/9x}}{x^{2/3}}-\frac{e^{-u^3/9(1-x)}}{(1-x)^{2/3}}\right]P(0,u).\end{aligned} \tag{B2}$$

To solve integral equation (B2) for the unknown function on the left-hand side, it is useful to consider the related integral equation

$$\int_0^1 dy\,\frac{R(y,u)}{|x-y|^{2/3}}=F(x,u). \tag{B3}$$

Making the replacements $x \to 1-x$ and $y \to 1-y$, one sees that any solution of Eq. (B3) also satisfies

$$\int_0^1 dy \, \frac{R(y,u)-R(1-y,u)}{|x-y|^{2/3}} = F(x,u) - F(1-x,u) \tag{B4}$$

Comparing Eqs. (B2) and (B4), recalling Eq. (10), and choosing

$$F(x,u) = x^{-2/3} e^{-u^3/9x}, \tag{B5}$$

we see that (B2) has the solution (7) in terms of $R(x,u)$.

Integral equation (B3) can be solved by factoring the kernel into two Volterra adjoint operators and has the solution [4,11]

$$R(x,u) = -3^{-1/2} \Gamma\left(\frac{1}{3}\right)^{-1} \Gamma\left(\frac{5}{6}\right)^{-2} x^{-1/6} \frac{d}{dx} \times \int_x^1 dy \, \frac{y^{1/3}}{(y-x)^{1/6}} \frac{d}{dy} \int_0^y dz \, \frac{F(z,u)}{z^{1/6}(y-z)^{1/6}}. \tag{B6}$$

Substituting Eq. (B5) into (B6) and evaluating the integrals with the help of [6], we obtain Eq. (8) for $R(x,u)$.

[1] S.J. Cornell, M.R. Swift, and A.J. Bray, Phys. Rev. Lett. **81**, 1142 (1998).

[2] M.R. Swift and A.J. Bray, Phys. Rev. E **59**, R4721 (1999).

[3] At $x=0$ the incident probability current with velocity between v_i and $v_i + dv_i$ equals the reflected probability current with velocity between v_f and $v_f + dv_f$. Thus $P(0,v_i) v_i dv_i = P(0,v_f) v_f dv_f$, which, together with $v_f = -r v_i$, implies Eq. (5).

[4] J. Masoliver and J.M. Porrà, Phys. Rev. Lett. **75**, 189 (1995); Phys. Rev. E **53**, 2243 (1996). The free energy of a semiflexible polymer in a tube is calulated with a related approach in T.W. Burkhardt, J. Phys. A **30**, L167 (1997).

[5] *Handbook of Mathematical Functions*, edited by M. Abramowitz and I.A. Stegun (Dover, New York, 1965).

[6] I.S. Gradshteyn and I.M. Ryzhik, *Tables of Integrals, Series, and Products* (Academic, New York, 1980).

[7] We use the standard notation ${}_pF_q(a_1, \ldots, a_p; b_1, \ldots, b_q; z) = \Sigma_{n=0}^{\infty}[(a_1)_n \ldots (a_p)_n/(b_1)_n \ldots (b_q)_n n!] z^n$, where $(c)_n = \Gamma(c+n)/\Gamma(c)$, for hypergeometric functions [6].

[8] Suppose that the particle is always reflected with the same velocities v_0 at $x=0$ and $-v_0$ at $x=1$, independent of the velocity just before striking the boundary. This is a variant of the half-space albedo problem solved by Cornell, Swift, and Bray [1]. The exact equilibrium distribution $P(x,v)$ on the interval $0<x<1$ is given by Eqs. (6)–(8) with $P(0,v) = \text{const} \times \delta(v-v_0)$.

[9] P.M. Morse and H. Feshbach, *Methods of Theoretical Physics* (McGraw-Hill, New York, 1953).

[10] G.E. Roberts and H. Kaufman, *Table of Laplace Transforms* (Saunders, Philadelphia, 1966).

[11] D. Porter and D.S.G. Stirling, *Integral Equations* (Cambridge University Press, Cambridge, 1990).